



UNIVERSITY OF LEEDS

This is a repository copy of *Iron(II) complexes of 2,6-di(1H-pyrazol-3-yl)-pyridine derivatives with hydrogen bonding and sterically bulky substituents.*

White Rose Research Online URL for this paper:  
<http://eprints.whiterose.ac.uk/83007/>

Version: Accepted Version

---

**Article:**

Roberts, TD, Little, M, Kershaw Cook, L et al. (1 more author) (2014) Iron(II) complexes of 2,6-di(1H-pyrazol-3-yl)-pyridine derivatives with hydrogen bonding and sterically bulky substituents. *Dalton Transactions*, 43 (20). 7577 - 7588. ISSN 1477-9226

<https://doi.org/10.1039/c4dt00355a>

---

**Reuse**

Items deposited in White Rose Research Online are protected by copyright, with all rights reserved unless indicated otherwise. They may be downloaded and/or printed for private study, or other acts as permitted by national copyright laws. The publisher or other rights holders may allow further reproduction and re-use of the full text version. This is indicated by the licence information on the White Rose Research Online record for the item.

**Takedown**

If you consider content in White Rose Research Online to be in breach of UK law, please notify us by emailing [eprints@whiterose.ac.uk](mailto:eprints@whiterose.ac.uk) including the URL of the record and the reason for the withdrawal request.



[eprints@whiterose.ac.uk](mailto:eprints@whiterose.ac.uk)  
<https://eprints.whiterose.ac.uk/>

# Iron(II) Complexes of 2,6-Di(1*H*-pyrazol-3-yl)-pyridine Derivatives with Hydrogen Bonding and Sterically Bulky Substituents†

Thomas D. Roberts<sup>a</sup>, Marc A. Little<sup>a,b</sup>, Laurence J. Kershaw Cook<sup>a</sup> and Malcolm A. Halcrow<sup>\*a</sup>

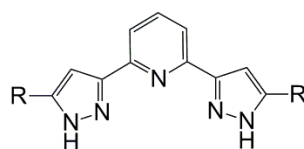
Syntheses of 2,6-di(5-aminopyrazol-3-yl)pyridine ( $L^1$ ), 2,6-di(5-*tert*butylcarboxamido-pyrazol-3-yl)pyridine ( $L^2$ ), 2,6-di(5-*tert*butylpyrazol-3-yl)pyridine ( $L^3$ ), 2-(5-*tert*butylpyrazol-3-yl)-6-(5-methylpyrazol-3-yl)pyridine ( $L^4$ ) and 2-(5-*tert*butylpyrazol-3-yl)-6-(5-amino-pyrazol-3-yl)pyridine ( $L^5$ ) are reported. Iron complex salts of the first four ligands were crystallographically characterised. The structures exhibit intermolecular hydrogen bonding between the cations and the anions and/or solvent, leading to a fluorite (**flu**) net, a 1D ladder structure, and a homochiral self-penetrating helical network related to the (10,3)-a (**srs**) topology. All the complexes are high-spin in the crystal, and bulk samples are also fully or predominantly high-spin at room temperature and below although two of the dried materials exhibit partial spin-state transitions on cooling.

## Introduction

Spin-crossover materials continue to be of great current interest,<sup>1-7</sup> for their application as switching centres in devices and in nanoscience<sup>3</sup> as well as for the more fundamental aspects of their structural chemistry<sup>4,5</sup> and physics.<sup>6</sup> Among the well-studied spin-crossover centres,  $[\text{Fe}(\text{3-bpp})_2]^{2+}$  (Scheme 1) is unusual because of its hydrogen bonding capability, containing Lewis acidic N–H groups directly adjacent to four of its six Fe–N bonds.<sup>8,9</sup> The proximity of these two functionalities makes the iron centre in  $[\text{Fe}(\text{3-bpp})_2]^{2+}$  unusually sensitive to changes in its hydrogen bonding. For example, hydrogen bonding to water strongly stabilises the low spin state of the complex, in the solid state<sup>10,11</sup> and in solution.<sup>12</sup> The solution-phase spin-equilibrium in  $[\text{Fe}(\text{3-bpp})_2]^{2+}$  is similarly responsive to the presence of different anions,<sup>13</sup> while cation...anion hydrogen bonding may also play a role in the cooperative spin-crossover transitions shown by some  $[\text{Fe}(\text{3-bpp})_2]^{2+}$  salts.<sup>8</sup>

While  $[\text{Fe}(\text{3-bpp})_2]^{2+}$  itself has been well studied, the synthesis of substituted analogues of 3-bpp is poorly developed. A number of 5,5'-disubstituted 3-bpp derivatives (Scheme 1,  $R = R' \neq \text{H}$ ) have been reported in recent years,<sup>9</sup> and studied for catalysis and small molecule activation,<sup>14</sup> as components in dye-sensitised solar cells,<sup>15</sup> and in self-assembly systems.<sup>16</sup> However, few of these have thus far been applied to spin-crossover chemistry,<sup>11,17</sup> which is surprising given the unusual chemistry of  $[\text{Fe}(\text{3-bpp})_2]^{2+}$  itself.

We now report iron(II) complexes of derivatives of 3-bpp, bearing substituents intended to promote hydrogen bonding between the coordinated ligand and peripheral anions or solvent (Scheme 1). These include additional protic substituents, designed to convert the pyrazolyl N–H functions into  $R_2(6)^{18}$  bifurcated hydrogen bond donor sites ( $L^1$ ,  $L^2$ );<sup>19,20</sup> bulky, hydrophobic *tert*butyl substituents, which we have previously found to promote novel metal/pyrazole assembly structures ( $L^3$ ,  $L^4$ );<sup>21-23</sup> and, a combination of the two ( $L^5$ ). Ligands  $L^4$  and  $L^5$  are the first examples of 3-bpp derivatives bearing an unsymmetric pattern of pyrazole substituents (Scheme 1,  $R \neq R'$ ).



$R = R' = \text{H}$ , 3-bpp  
 $R = R' = \text{NH}_2$ ,  $L^1$   
 $R = R' = \text{NHC(O)tBu}$ ,  $L^2$   
 $R = R' = \text{tBu}$ ,  $L^3$   
 $R = \text{tBu}$ ,  $R' = \text{Me}$ ,  $L^4$   
 $R = \text{tBu}$ ,  $R' = \text{NH}_2$ ,  $L^5$

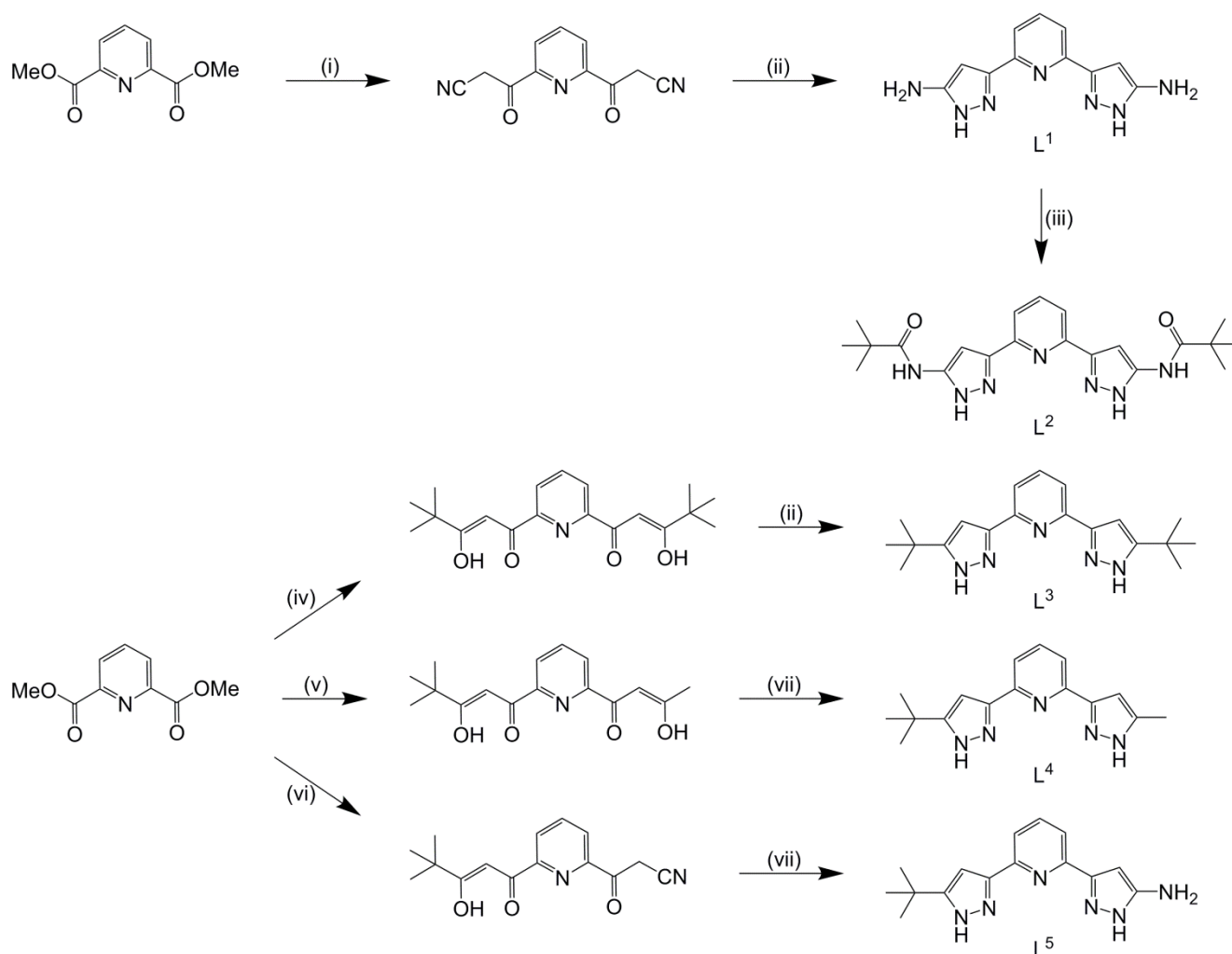
Scheme 1 Ligands referred to in this work.

## Results and Discussion

Ligands  $L^1$  and  $L^3$  were prepared in two steps from 2,6-diacetylpyridine, by modifications of the literature procedures

(Scheme 2).<sup>24,25</sup> Treatment of  $L^1$  with pinacol chloride in acetonitrile precipitated the hydrochloride salt of  $L^2$ , which was converted to its free base with aqueous  $\text{Na}_2\text{CO}_3$ .<sup>19</sup> Reactions of  $L^1$  with acyl or benzoyl chloride also yielded the corresponding di(methylamido) or di(phenylamido) derivatives, which unfortunately proved too insoluble for use in complexation studies. In our hands the first step in the synthesis of  $L^3$ , a double Claisen condensation reaction,<sup>25</sup> was sluggish and yielded significant amounts of the singly condensed byproduct

as well as the expected *bis*( $\beta$ -diketone) shown in Scheme 2. These compounds are always produced together and could not be separated by column chromatography, which may account for the low yield of  $L^3$  obtained by this route. However, adjusting the reaction conditions allows the mono-condensate to be obtained as the major product, which was then employed *in situ* in a second Claisen or Knoevenagel condensation step. Hydrazinolysis of the resultant unsymmetric  $\beta$ -diketones affords  $L^4$  and  $L^5$  (Scheme 2).



**Scheme 2** Syntheses of the ligands in this work. Experimental conditions: (i) NaH (2 eq), MeCN (2 eq), THF, reflux. (ii)  $\text{N}_2\text{H}_4 \cdot \text{H}_2\text{O}$ , EtOH, reflux. (iii) *t*BuCOCl, MeCN then  $\text{Na}_2\text{CO}_3$  (aq). (iv) NaOEt (2 eq), *t*BuCOMe (2 eq), toluene then  $\text{MeCO}_2\text{H}$ ,  $\text{H}_2\text{O}$ . (v) NaOMe (1 eq), *t*BuCOMe (1 eq), toluene then NaOMe (1.5 eq),  $\text{Me}_2\text{CO}$  (1 eq), toluene. (vi) NaOMe (1 eq), *t*BuCOMe (1 eq), toluene; NaH (1 eq), MeCN (1 eq), toluene; then, HCl (aq). (vii)  $\text{N}_2\text{H}_4 \cdot \text{H}_2\text{O}$ , EtOH: $\text{MeCO}_2\text{H}$ , rt.

The complexes  $[\text{FeL}_2]\text{X}_2$  ( $L = L^1$ ,  $1\text{X}_2$ ;  $L = L^2$ ,  $2\text{X}_2$ ;  $L = L^3$ ,  $3\text{X}_2$ ;  $L = L^4$ ,  $4\text{X}_2$ ;  $X^- = \text{BF}_4^-$  or  $\text{ClO}_4^-$ ) were obtained by treatment of the appropriate hydrated iron(II) salt with 2 equiv of the ligand in nitromethane or methanol. The complexes are soluble in the usual solvents expected for dicationic complex salts, namely MeCN,  $\text{MeNO}_2$ ,  $\text{CF}_3\text{CH}_2\text{OH}$  and in some cases acetone and methanol. Extensive crystallisation experiments with different solvent:antisolvent combinations yielded the

single crystal materials described below. No diffraction quality crystals were obtained from salts of  $[\text{Fe}(L^5)_2]^{2+}$ , so that complex was not pursued further. Salts of  $1^{2+}$  are air sensitive in organic solvents and the solid state, as evidenced by a colour change from yellow to dark green. Although we have not been able to unambiguously identify the decomposition product, precedent suggests it may be an iron(III) complex with deprotonated  $L^1$  ligand(s).<sup>26,27</sup> Notably none of the other complexes in this work,

or  $[\text{Fe}(\text{3-bpp})_2]^{2+}$  itself, is comparably sensitive. The air-sensitivity of  $1^{2+}$  may reflect the greater basicity of the aminopyrazolyl donor groups in  $L^1$  compared to the other ligand pyrazole substituents in this study,<sup>28</sup> which would lower its Fe(II/III) oxidation potential.

While several salts of  $1^{2+}$  were examined, only  $1[\text{ClO}_4]_2$  was found to form single crystals, from nitromethane/diethyl ether mixtures. The complex was more stable in crystalline form than as a powder, which facilitated its characterisation, but the crystals still darkens in air over a period of hours. The crystals, of formula  $1[\text{ClO}_4]_2 \cdot 2(\text{C}_2\text{H}_5)_2\text{O} \cdot \text{CH}_3\text{NO}_2$ , contain half a complex dication spanning a crystallographic  $C_2$  axis (Fig. 1). One 5-aminopyrazolyl domain of the unique  $L^1$  ligand chelates to the perchlorate ion in a  $R_3^2(8)$  ring motif<sup>18</sup> and donates a bifurcated hydrogen bond interaction to another, symmetry related anion site. The other 5-aminopyrazolyl residue hydrogen bonds to the unique diethyl ether molecule through its pyrazole N–H group, while its amino function donates single hydrogen bonds to two other perchlorate sites. Each  $L^1$  ligand hydrogen bonds to four different anions in total, and the  $C_2$ -symmetric cation is thus eight-connected in topological terms with a puckered cubic arrangement of nearest neighbour anions.

The  $\text{ClO}_4^-$  anions are all crystallographically equivalent and four-connected, in a flattened tetrahedral geometry. This results in a distorted version of the fluorite [**flu**,  $(4^6)(4^{12}6^{12}8^4)$ ] topology hydrogen bond network (Fig. 2).<sup>29</sup> The flu network is unusual in molecular crystals because of its eight-connected

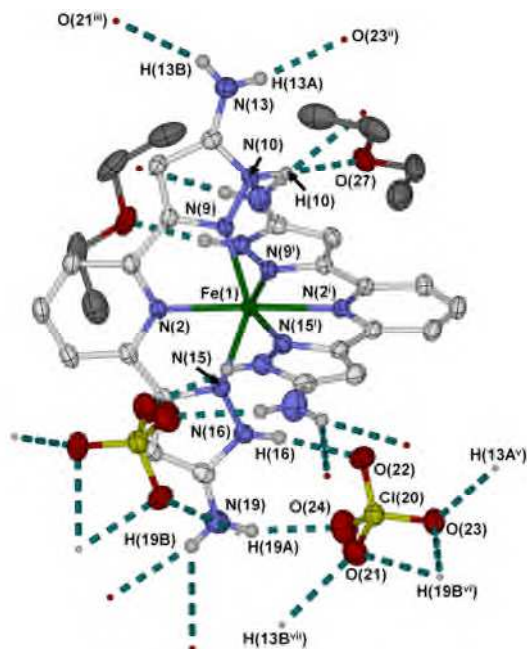


**Fig. 1.** The formula unit in  $1[\text{ClO}_4]_2 \cdot 2(\text{C}_2\text{H}_5)_2\text{O} \cdot \text{CH}_3\text{NO}_2$ , showing the hydrogen bonding in the lattice. The disordered nitromethane residue, which does not take part in hydrogen bonding, is not shown. Atomic displacement ellipsoids are at the 50 % probability level, and C-bound H atoms have been omitted. Colour code: C {complex}, white; C {solvent}, dark grey; H, grey; Cl, yellow; Fe, green; N, pale blue; O, red. Symmetry codes: (i)  $1-x, y, 1/2-z$ ; (ii)  $1/2+x, 3/2-y, -z$ ; (iii)  $1/2+x, 1/2+y, 1/2-z$ ; (iv)  $x, -1+y, 1/2+z$ ; (v)  $-1/2+x, 3/2-y, -z$ ; (vi)  $x, 1-y, -1/2+z$ ; (vii)  $-1/2+x, -1/2+y, 1/2-z$ .

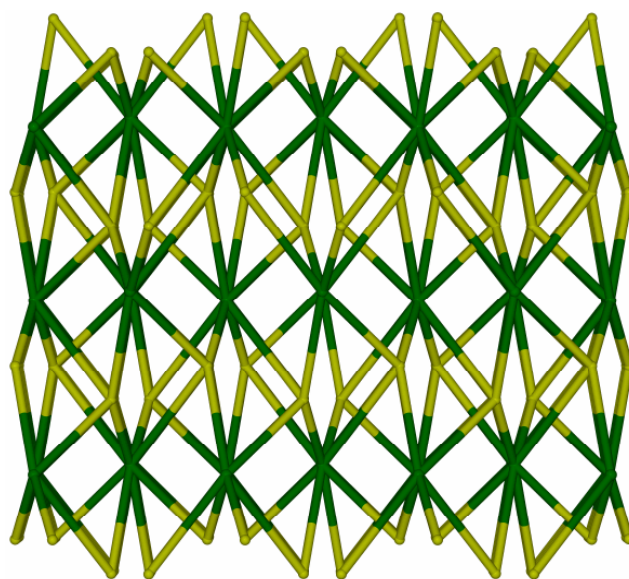


**Fig. 2.** Fragment of the distorted **flu** hydrogen bond network in  $1[\text{ClO}_4]_2 \cdot 2(\text{C}_2\text{H}_5)_2\text{O} \cdot \text{CH}_3\text{NO}_2$ . Connections between the centres of the hydrogen bonded cations (green) and anions (yellow) are shown. The view is parallel to the crystallographic (100) vector, with  $c$  horizontal.

nodes, but it has been seen before in coordination polymers<sup>30</sup> and a hydrogen bonded lattice.<sup>31</sup> The eight-connected nodes in most of these literature structures are polymetallic clusters, however, in contrast to the mononuclear complex in  $1[\text{ClO}_4]_2 \cdot 2(\text{C}_2\text{H}_5)_2\text{O} \cdot \text{CH}_3\text{NO}_2$ .

Crystals of  $2[\text{BF}_4]_2 \cdot 3\text{CH}_3\text{CN}$  and  $2[\text{ClO}_4]_2 \cdot 3\text{CH}_3\text{CN}$  are isostructural, with asymmetric units containing one formula unit lying on a general crystallographic site (Fig. 3). One of the four carboxamido groups, N(13), is *syn* to its bound pyrazolyl N–H function N(10), and chelates to a tetrahedral anion in the lattice. The other three 5-(carboxamido)-1*H*-pyrazolyl groups in the molecule adopt an *anti* conformation. These amido N–H groups each hydrogen bond to an anion, while the pyrazolyl N–H group forms an intramolecular interaction to its neighbouring carbonyl O atom and, in two cases, to an acetonitrile molecule. These interactions lead to a 1D hydrogen bonded array with a ladder topology, running parallel to the crystallographic  $a$  axis (ESI†).

The asymmetric unit of  $3[\text{BF}_4]_2 \cdot x\text{CF}_3\text{CH}_2\text{OH} \cdot y(\text{C}_3\text{H}_7)_2\text{O}$  contains two formula units of the compound ( $Z' = 2$ ; Fig. 4). The unique complex molecules are broadly similar but differ in the conformations of the  $L^3$  ligand backbones, which are twisted into an S-shaped conformation. This distortion is more pronounced in molecule A, where the intra-ligand dihedral angles between the least squares planes of the pyridine and pyrazole rings range from  $6.8(4)$ – $15.9(3)^\circ$ , than in molecule B [ $3.7(3)$ – $8.5(3)^\circ$ ]. It may be a consequence of some close intermolecular contacts in the lattice, which are oriented to displace the pyrazolyl groups from the plane of the ligand as observed (ESI†).<sup>32</sup> Although many of these contacts involve *tert*butyl groups, there are no equivalent conformational distortions in the salts of  $2^{2+}$  (see above).

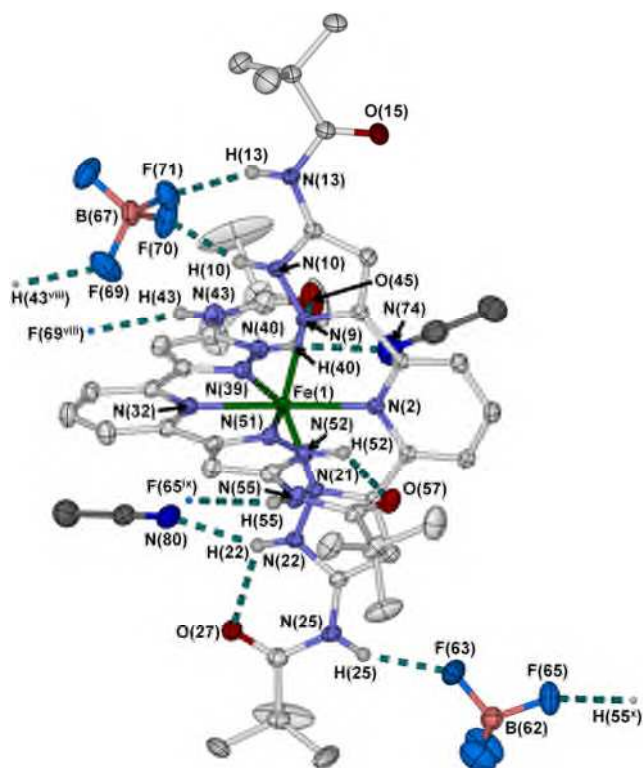


**Fig. 3.** The formula unit in  $2[\text{BF}_4]_2 \cdot 3\text{CH}_3\text{CN}$ , showing the hydrogen bonding in the lattice. One solvent molecule that does not take part in hydrogen bonding is not shown. Atomic displacement ellipsoids are at the 50% probability level, and C-bound H atoms have been omitted. Colour code: C {complex}, white; C {solvent}, dark grey; H, grey; B, pink; F, cyan; Fe, green; N {complex}, pale blue; N {solvent}, dark blue; O, red. Symmetry codes: (viii)  $-x, -y, -z$ ; (ix)  $-1+x, y, z$ ; (x)  $1+x, y, z$ .

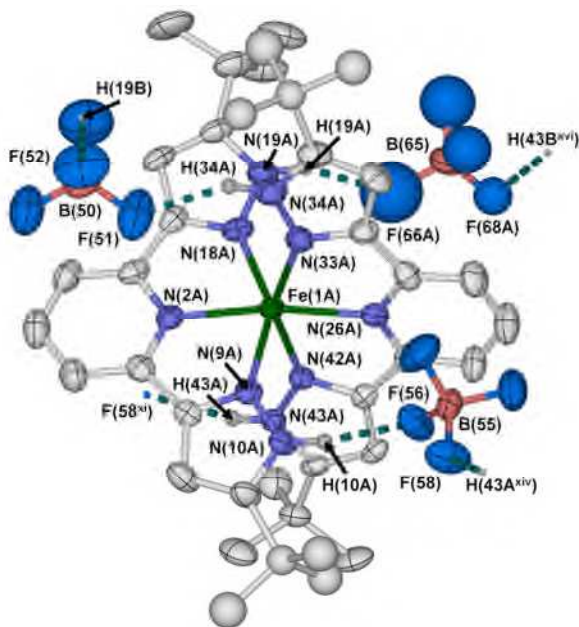


**Fig. 4.** Complex molecule A in  $3[\text{BF}_4]_2 \cdot x\text{CF}_3\text{CH}_2\text{OH} \cdot y(\text{C}_3\text{H}_7)_2\text{O}$ , and its associated  $\text{BF}_4^-$  ions. Atomic displacement ellipsoids are at the 50% probability level, and C-bound H atoms have been omitted and only one orientation of the disordered *tert*butyl groups and  $\text{BF}_4^-$  ion are shown. Colour code: C, white; H, grey; B, pink; F, cyan; Fe, green; N, pale blue. Symmetry codes: (xi)  $1-x, 1/2+y, 1/2-z$ ; (xiv)  $1-x, -1/2+y, 1/2-z$ ; (xvi)  $1/2-x, 1-y, 1/2+z$ .

Both molecules form four monodentate N–H...F hydrogen bonds to  $\text{BF}_4^-$  ions, with all four anions hydrogen bonding to two different complex cations. Topologically, therefore, molecules A and B are both four-connected centres, linking to four complex molecule neighbours through two-connected bridging anions. Each complex node has two connections to neighbouring molecules of the same type (A...A or B...B), and two A...B connections that are crystallographically distinct, but almost equal in length. The A...B connections form four-fold helices parallel to the *c*-axis, with alternating A and B vertices. These helices all have the same handedness, and have  $\Delta$  helicity in the crystal that was measured. The A...A and B...B connections then link each pair of helices into a four-fold array, in a self-penetrating manner (Fig. 5). The overall topology is related to the (10,3)-a [srs] three-connected helical net, but with the co-parallel connections between each helix in srs being replaced by twice the number of interweaving linkages (ESI<sup>†</sup>).<sup>29</sup> While interpenetrating structures comprised of distinct, entangled srs nets are well known,<sup>33</sup> this is a new self-penetrating modification of a single srs topology.

Lastly,  $4[\text{BF}_4]_2 \cdot x\text{CF}_3\text{CH}_2\text{OH} \cdot y(\text{C}_2\text{H}_5)_2\text{O}$  contains one unique molecule per asymmetric unit. The two 5-methylpyrazolyl groups in the complex both donate N–H...F hydrogen bonds to a  $\text{BF}_4^-$  ion, while the 5-*tert*butylpyrazolyl residues

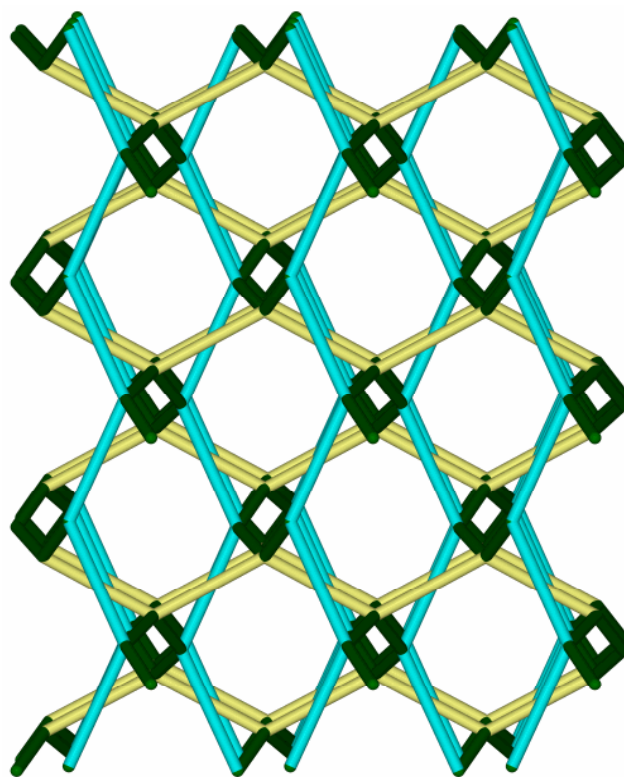


**Fig. 5.** Fragment of the interpenetrating helical hydrogen bond network in  $3[\text{BF}_4]_2 \cdot x\text{CF}_3\text{CH}_2\text{OH} \cdot y(\text{C}_3\text{H}_7)_2\text{O}$ . The A...B connections forming the helices are green, the while A...A (cyan) and B...B (yellow) connections link the helices in a self-penetrating manner. The view is approximately parallel to the crystallographic (001) vector, with *a* horizontal.

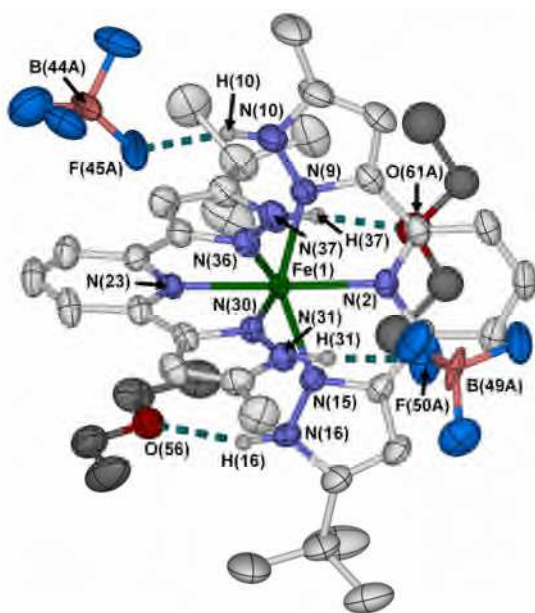


**Fig. 6.** View of the hydrogen bonded assembly in  $4[\text{BF}_4]_2 \cdot x\text{CF}_3\text{CH}_2\text{OH} \cdot y(\text{C}_2\text{H}_5)_2\text{O}$ . Atomic displacement ellipsoids are at the 50 % probability level, C-bound H atoms have been omitted, and only one orientation of the disordered  $\text{BF}_4^-$  ions and solvent are shown. Colour code: C (complex), white; C (solvent), dark grey; H, grey; B, pink; F, cyan; Fe, green; N, pale blue; O, red.

form N–H...O interactions to diethyl ether molecules. None of these interactions leads to bridging between molecules, and the crystals are composed of discrete  $\{[\text{Fe}(\text{L}^4)_2]^{2+} \cdot 2[\text{BF}_4]^- \cdot 2(\text{C}_2\text{H}_5)_2\text{O}\}$  assemblies (Fig. 6).

The iron centres in all these crystals are high-spin at the temperature of measurement (110 K for  $4[\text{BF}_4]_2$ , 150 K for the other compounds) according to their metric parameters (Table

1). The coordination geometries of  $1[\text{ClO}_4]_2$  and  $4[\text{BF}_4]_2$  show only small deviations from  $D_{2d}$  symmetry, if their peripheral substituents are not considered. However, the iron centres in the salts of  $2^{2+}$  and  $3[\text{BF}_4]_2$  are strongly distorted, which is characteristic of an angular Jahn-Teller distortion that is sometimes exhibited by high-spin complexes of meridional *tris*-imine ligands.<sup>34</sup> This results in a *trans*-N(pyridyl)–Fe–N(pyridyl) angle ( $\phi$ ) lower than its ideal value of  $180^\circ$ , and/or a twisting of the ligands from the perpendicular ( $\theta < 90^\circ$ , where  $\theta$  is the dihedral angle between the least-squares planes of the two ligands). Distorted complexes cannot exhibit spin-crossover to their (undistorted) low-spin forms in the solid state, since a rigid lattice cannot accommodate the resultant structural changes. This distortion is unusual in compounds from the  $[\text{Fe}(\text{3-bpp})_2]^{2+}$  series,<sup>35</sup> but is common in high-spin  $[\text{Fe}(\text{1-bpp})_2]^{2+}$  (1-bpp = 2,6-di{pyrazol-1-yl}pyridine, an isomer of 3-bpp)<sup>34,36</sup> and  $[\text{Fe}(\text{terpy})_2]^{2+}$  derivatives.<sup>37</sup>

In  $2[\text{BF}_4]_2$  and  $2[\text{ClO}_4]_2$ , the ligands are perpendicular to each other ( $\theta \approx 90^\circ$ ), but  $\phi$  is strongly reduced to  $158\text{--}159^\circ$ . In contrast, the two unique molecules of  $3[\text{BF}_4]_2$  show  $\phi = 170\text{--}172^\circ$ , closer to its ideal value, but lower values of  $\theta$  (68 and  $71^\circ$ ). Both distortions are within precedent, and are of a magnitude that would normally prohibit thermal spin-crossover.<sup>36</sup> The more regular coordination geometries of  $1[\text{ClO}_4]_2$  and  $4[\text{BF}_4]_2$  should not, in themselves, inhibit a thermal spin-transition however. These observations are consistent with the spin-states adopted by bulk samples of the compounds, described below.

All the salts of  $1^{2+}\text{--}4^{2+}$  afford yellow powders after drying *in vacuo*, which retain some solvent or atmospheric moisture by microanalysis. Solid  $2[\text{BF}_4]_2 \cdot \text{H}_2\text{O}$ ,  $2[\text{ClO}_4]_2 \cdot 2\text{H}_2\text{O}$  and  $3[\text{BF}_4]_2 \cdot \text{CF}_3\text{CH}_2\text{OH}$  are all high-spin between 5–300 K (ESI<sup>†</sup>), which is consistent with their crystal structures. However,

**Table 1** Selected structural parameters for the crystal structures in this work ( $\text{\AA}$ ,  $^\circ$ ).  $\alpha$ ,  $\Sigma$  and  $\Theta$  are indices showing the spin state of the complex,<sup>38</sup> while  $\theta$  and  $\phi$  are measures of the angular Jahn-Teller distortion sometimes shown by this type of iron center in its high-spin state.<sup>34,36</sup> Typical values of these parameters in  $[\text{Fe}(\text{bpp})_2]^{2+}$  derivatives are given in ref. 36, and more complete tables of bond lengths and angles for the structures are in the ESI<sup>†</sup>.

	$1[\text{ClO}_4]_2 \cdot 2(\text{C}_2\text{H}_5)_2\text{O} \cdot \text{CH}_3\text{NO}_2^a$	$2[\text{BF}_4]_2 \cdot 3\text{CH}_3\text{CN}$	$2[\text{ClO}_4]_2 \cdot 3\text{CH}_3\text{CN}$
Fe–N{pyridyl}	2.1567(12)	2.1333(11), 2.1562(11)	2.134(2), 2.163(2)
Fe–N{pyrazolyl}	2.1888(13), 2.1936(12)	2.1654(11)–2.2214(11)	2.174(2)–2.2291(18)
$\alpha$	73.43(7)	73.81(8)	73.88(15)
$\Sigma$	151.2(2)	152.7(1)	151.4(2)
$\Theta$	464	462	460
$\phi$	177.33(6)	158.30(4)	158.91(7)
$\theta$	87.91(1)	89.67(1)	89.01(2)
	$3[\text{BF}_4]_2 \cdot x\text{CF}_3\text{CH}_2\text{OH} \cdot y(\text{C}_3\text{H}_7)_2\text{O}^b$		$4[\text{BF}_4]_2 \cdot x\text{CF}_3\text{CH}_2\text{OH} \cdot y(\text{C}_2\text{H}_5)_2\text{O}$
	Molecule A	Molecule B	
Fe–N{pyridyl}	2.129(4), 2.146(4)	2.166(3), 2.170(3)	2.116(3), 2.119(3)
Fe–N{pyrazolyl}	2.183(4)–2.224(3)	2.202(3)–2.271(3)	2.184(3)–2.188(3)
$\alpha$	74.2(3)	73.6(3)	74.5(2)
$\Sigma$	158.5(5)	172.1(4)	140.1(4)
$\Theta$	448	468	438
$\phi$	170.27(13)	171.85(13)	174.33(10)
$\theta$	68.02(5)	71.46(4)	88.85(3)

<sup>a</sup>The asymmetric unit of this compound contains half a complex molecule, with crystallographic  $C_2$  symmetry. <sup>b</sup>The asymmetric unit of this compound contains two unique complex molecules.

$4[\text{BF}_4]_2 \cdot \frac{1}{2}\text{CF}_3\text{CH}_2\text{OH}$  exhibits a continuous decrease in its magnetic moment, from  $\chi_M T = 3.6 \text{ cm}^3\text{mol}^{-1}\text{K}$  at 300 K (100 % high-spin) to  $2.1 \text{ cm}^3\text{mol}^{-1}\text{K}$  at 50 K (ca. 60:40 high:low-spin population). That is inconsistent with its high-spin crystal structure at 110 K, although the coordination geometry of the complex could accommodate a spin-transition in principle. Freshly prepared  $4[\text{BF}_4]_2 \cdot x\text{CF}_3\text{CH}_2\text{OH} \cdot y(\text{C}_2\text{H}_5)_2\text{O}$  may remain high-spin at low temperatures because of a crowded steric environment around the cations in the lattice, inhibiting the structural changes associated with spin-crossover.<sup>4</sup> Partial removal of the solvent would create voids in the lattice, alleviating steric crowding and permitting a fraction of the sample to undergo spin-crossover, as observed. Lastly, bulk samples of  $1[\text{ClO}_4]_2 \cdot 2\text{H}_2\text{O}$  show mixed behaviour. Most of the material remains high-spin on cooling, which is consistent with the crystallography, but this is superimposed upon an abrupt spin-transition near 160 K that is undergone by 25-30 % of the iron centres (ESI†). This behaviour is reproducible between samples. We have been unable to isolate the spin-crossover phase of  $1[\text{ClO}_4]_2$  from the rest of the material, and we tentatively suggest that it may be a decomposition product from the air-sensitive complex.<sup>39</sup>

## Conclusions

This study has investigated the structural chemistry of five new  $[\text{Fe}(\text{3-bpp})_2]^{2+}$  derivatives, bearing hydrogen bonding or sterically bulky substituents adjacent to their distal N–H groups. In keeping with other 5-aminopyrazole chelate complexes,<sup>19,20</sup> salts of  $1^{2+}$  and  $2^{2+}$  show extensive hydrogen bonding to anions and solvent, and can chelate inorganic anions in the crystal. Strong hydrogen bonding is also observed in  $3[\text{BF}_4]_2$ , despite the bulky *tert*butyl groups shielding the pyrazolyl N–H groups. The hydrogen bond networks exhibited by these crystals include an unusual **flu** net and a unique self-penetrating helical topology.

A goal of this work was to use this enhanced hydrogen bonding to produce spin-crossover materials showing cooperative switching behaviour.<sup>4</sup> However, apart from minor fractions of  $1[\text{ClO}_4]_2 \cdot 2\text{H}_2\text{O}$  and  $4[\text{BF}_4]_2 \cdot \frac{1}{2}\text{CF}_3\text{CH}_2\text{OH}$ , which are of uncertain origin, none of these compounds exhibits a thermal spin-transition (ESI†). In some cases that reflects their adoption of a Jahn-Teller distorted structure that is known to inhibit spin-crossover.<sup>34,36</sup> However the electron-withdrawing character of the amido substituents in  $2^{2+}$  (which will stabilise the high-spin state), and the bulk of the *tert*butyl groups in  $2^{2+}$ - $4^{2+}$  (producing a sterically crowded crystal lattice), could also contribute to the observed behaviour. Since other pyrazole-substituted derivatives of  $[\text{Fe}(\text{3-bpp})_2]^{2+}$  are spin crossover-active,<sup>11,17</sup> we are continuing to investigate other methods to enhance hydrogen bonding in this complex type.

Finally, another feature of this study is the synthesis of  $\text{L}^4$  and  $\text{L}^5$ , the first 3-bpp derivatives bearing an unsymmetric pattern of pyrazole substituents.<sup>9</sup> The method depends on the slow Claisen condensation between pinacolone and dimethyl pyridine-2,6-dicarboxylate, and so may not be applicable for all

substituent combinations. However, it could be used to make other 5,5'-disubstituted 3-bpp derivatives containing just one *tert*butyl group (Scheme 1;  $\text{R} = t\text{Bu}$ ,  $\text{R}' = \text{any substituent}$ ), which could be of value for catalysis<sup>14</sup> and photosensitiser applications<sup>15</sup> as well as for SCO.

## Experimental

Unless otherwise stated, all reactions were carried out in air using as-supplied AR-grade solvents. Other reagents and solvents were purchased commercially and used as supplied.

**CAUTION.** While we have experienced no difficulties with  $1[\text{ClO}_4]_2$  and  $2[\text{ClO}_4]_2$ , as metal-organic perchlorates they are potentially explosive and should be handled with care in small quantities.

**Synthesis of 2,6-di(2-cyanoacetyl)pyridine.**<sup>24</sup> Dimethyl pyridine-2,6-dicarboxylate (25.0 g, 130 mmol) and acetonitrile (10.3 g, 320 mmol) were dissolved in dry THF (300  $\text{cm}^3$ ). Sodium hydride (60 wt % in mineral oil, 21.0 g, 530 mmol) was then added, and the mixture was heated at reflux for 2 hours, yielding a pale yellow solid that was collected by filtration. The solid was redissolved in water (400  $\text{cm}^3$ ) and the solution was acidified to pH 5. The resultant precipitate was filtered, washed with water, dried and re-crystallised from ethanol/dioxane to give the product as an orange solid. Yield 9.4 g, 34.4 %. Found C, 62.1; H, 3.30; N, 19.6 %. Calcd. for  $\text{C}_{11}\text{H}_7\text{O}_2\text{N}_3$  C, 62.0; H, 3.31; N, 19.7 %. ESMS  $m/z$  236.1 ( $[\text{M} + \text{Na}]^+$ ).  $^1\text{H}$  NMR ( $\{\text{CD}_3\}_2\text{CO}$ )  $\delta$  4.84 (s, 4H,  $\text{CH}_2$ ), 8.38 (s, 3H, Py  $\text{H}^{3-5}$ ).  $^{13}\text{C}$  NMR ( $\{\text{CD}_3\}_2\text{CO}$ )  $\delta$  28.6 (2C,  $\text{CH}_2$ ), 114.8 (2C,  $\text{C}\equiv\text{N}$ ), 125.8 (2C, Py  $\text{C}^{3/5}$ ), 139.4 (1C, Py  $\text{C}^4$ ), 150.0 (2C, Py  $\text{C}^{2/6}$ ), 189.3 (C=O).

**Synthesis of 2,6-di(5-amino-1H-pyrazol-3-yl)pyridine hemihydrate ( $\text{L}^1 \cdot \frac{1}{2}\text{H}_2\text{O}$ ).**<sup>24</sup> Hydrazine hydrate (9.0 g, 180 mmol) was added to a suspension of 2,6-di(2-cyanoacetyl)pyridine (8.0 g, 37 mmol) in ethanol (100  $\text{cm}^3$ ). The mixture was refluxed for 20 hrs, which gave an orange solution with a brown precipitate which was removed by filtration. The filtrate was reduced to 50 % volume and then diluted with diethyl ether (225  $\text{cm}^3$ ). The resultant precipitate was collected, washed with pentane and dried *in vacuo*. Yield 5.2 g, 57 %. Found C, 52.0; H, 4.75; N, 39.0 %. Calcd. for  $\text{C}_{11}\text{H}_{11}\text{N}_7 \cdot \frac{1}{2}\text{H}_2\text{O}$  C, 52.8; H, 4.83; N, 39.2 %. ESMS  $m/z$  242.1  $[\text{HL}]^+$ .  $^1\text{H}$  NMR ( $\{\text{CD}_3\}_2\text{SO}$ )  $\delta$  4.69 (br s, 4H,  $\text{NH}_2$ ), 6.09 (s, 2H, Pz  $\text{H}^4$ ), 7.55 (br s, 2H, Py  $\text{H}^5$ ), 7.82 (br s, 1H, Py  $\text{H}^4$ ), 12.16 (br s, 2H, Pz  $\text{NH}$ ).  $^{13}\text{C}$  NMR ( $\{\text{CD}_3\}_2\text{SO}$ )  $\delta$  90.0 (2C, Pz  $\text{C}^4$ ), 117.5 (2C, Py  $\text{C}^{3/5}$ ), 138.3 (1C, Py  $\text{C}^4$ ), 141.2 (Pz  $\text{C}^3$ ), 147.3 (Pz  $\text{C}^5$ ), 156.5 (Py  $\text{C}^{2/6}$ ).

**Synthesis of 2,6-bis(5-*tert*butylamido)-1H-pyrazol-3-yl)pyridine hemihydrate ( $\text{L}^2 \cdot \frac{1}{2}\text{H}_2\text{O}$ ).** Trimethylacetyl chloride (4.0 g, 33.2 mmol) was added to a stirred suspension of  $\text{L}^1$  (2.0 g, 8.3 mmol) in dry acetonitrile (90  $\text{cm}^3$ ) under a dinitrogen atmosphere. The mixture was refluxed for 48 hours, and the resultant white precipitate was collected by filtration

and dried in air. This solid was identified as the monohydrochloride salt of L<sup>2</sup> by microanalysis. Yield 2.8 g, 75 %. Found C, 56.3; H, 6.35; N, 22.2; Cl, 8.10 %. Calcd. for C<sub>21</sub>H<sub>27</sub>N<sub>7</sub>O<sub>2</sub>·HCl C, 56.6; H, 6.33; N, 22.0; Cl, 7.95 %. Saturated aqueous Na<sub>2</sub>CO<sub>3</sub> (150 cm<sup>3</sup>) was added to a suspension of L<sup>2</sup>·HCl (2.5 g, 5.6 mmol) in chloroform (150 cm<sup>3</sup>), and the mixture was heated to reflux for 72 hours. The two phase solution was cooled and separated. The aqueous layer was extracted with dichloromethane (2 x 30 cm<sup>3</sup>), and the organic fractions were combined with the original chloroform layer and evaporated to a white residue that was analysed without further purification. Yield 1.6 g, 71 %. Found C, 60.6; H, 6.65; N, 23.3 %. Calcd. for C<sub>21</sub>H<sub>27</sub>N<sub>7</sub>O<sub>2</sub>·½H<sub>2</sub>O C, 60.3; H, 6.74; N, 23.4 %. ESMS *m/z* 432.2 ([NaL<sup>2</sup>]<sup>+</sup>). <sup>1</sup>H NMR (CDCl<sub>3</sub>) δ 1.27 (s, 18H, CH<sub>3</sub>), 7.31 (br s, 2H, Pz H<sup>4</sup>), 7.46 (d, 7.2 Hz, 2H, Py H<sup>3/5</sup>), 7.71 (t, 6.2 Hz, 1H, Py H<sup>4</sup>) 8.86 (br s, 2H, NHCO), 12.41 (br s, 2H, Pz NH). <sup>13</sup>C NMR (CDCl<sub>3</sub>) δ 26.5 (CH<sub>3</sub>), 94.7 (Pz C<sup>4</sup>), 118.7 (Py C<sup>3</sup>), 137.2 (Py C<sup>4</sup>), 141.3, 146.4, 148.5 (Py C<sup>2/6</sup>, Pz C<sup>3</sup>, Pz C<sup>5</sup>), 175.6 (C=O).

**Synthesis of 2,6-bis(5-*tert*-butyl-1H-pyrazol-3-yl)pyridine methanol solvate (L<sup>3</sup>·CH<sub>3</sub>OH).**<sup>25</sup> Sodium ethoxide was prepared by stirring sodium (0.77 g, 33.4 mmol) in ethanol (15 cm<sup>3</sup>) until all the metal was consumed, and then removing the solvent *in vacuo*. Toluene (30 cm<sup>3</sup>) and pinacolone (3.9 g, 38.5 mmol) were added to the white residue, followed by dimethylpyridine-2,6-dicarboxylate (2.5 g, 12.8 mmol). The mixture was stirred for 8 hrs at room temperature, then for 4 hrs at 60° C. The red solution was evaporated to dryness and the residue added to a mixture of acetic acid (15 cm<sup>3</sup>), water (25 cm<sup>3</sup>) and ice (50 g). The mixture was filtered, and the precipitate was dried and dissolved in dichloromethane. The solution was washed with saturated aqueous Na<sub>2</sub>CO<sub>3</sub> (2 x 30 cm<sup>3</sup>) and water (30 cm<sup>3</sup>) before being dried (MgSO<sub>4</sub>) and the solvent removed to leave 1.4 g of an orange solid containing a mixture of I and II (Scheme 2). This crude material was dissolved in ethanol (40 cm<sup>3</sup>) and hydrazine monohydrate (0.60 g, 11.9 mmol) was added. The mixture was then heated at reflux for 16 hrs. Concentration of the cooled solution to half its original volume, and addition of water, yielded a white precipitate which was collected by filtration and dried. The desired product L<sup>3</sup> was purified from this material by silica column chromatography (9:1 ethyl acetate:methanol eluent). Yield 0.16 g, 12.7 %. Found C, 68.3; H, 7.80; N, 20.0 %. Calcd for C<sub>19</sub>H<sub>25</sub>N<sub>5</sub>·CH<sub>3</sub>OH C, 67.6; H, 8.22; N, 19.7 %. ESMS *m/z* 324.2 ([HL<sup>3</sup>]<sup>+</sup>). <sup>1</sup>H NMR (CDCl<sub>3</sub>) δ 1.35 (s, 18 H, C(CH<sub>3</sub>)<sub>3</sub>), 6.66 (s, 2 H, Pz H<sup>4</sup>), 7.62 (m, 3H, Py H<sup>3-5</sup>). <sup>13</sup>C NMR (CDCl<sub>3</sub>) δ 30.4 (6C, C(CH<sub>3</sub>)<sub>3</sub>), 30.9 (2C, C(CH<sub>3</sub>)<sub>3</sub>), 99.9 (2C, Pz C<sup>4</sup>), 118.6 (2C, Py C<sup>3/5</sup>), 137.4 (1C, Py C<sup>4</sup>), 146.0 (2C, Pz C<sup>3</sup>), 149.5 (2C, Pz C<sup>5</sup>), 159.7 (2C, Py C<sup>2/6</sup>).

**Synthesis of 2-(5-*tert*-butyl-1H-pyrazol-3-yl)-6-(5-methyl-1H-pyrazol-3-yl)pyridine (L<sup>4</sup>).** Dimethyl pyridine-2,6-dicarboxylate (3.0 g, 18.4 mmol) and sodium methoxide (1.0 g, 18.4 mmol) were suspended in dry toluene (350 cm<sup>3</sup>) under a dinitrogen atmosphere. Pinacolone (1.8 g, 18.4 mmol) was then

added and the mixture was heated at 70 °C for 48 hrs. The red mixture was then cooled and acetone (0.80 g, 13.7 mmol) was added, followed by more sodium methoxide (1.1 g, 20.5 mmol). The mixture was then heated at 70 °C for a further 72 hours. The mixture was cooled, affording 1.5 g of 2-(3-hydroxy-4,4-dimethylpent-2-enoyl)-6-(3-hydroxypent-2-enoyl)pyridine as a yellow precipitate which was collected by filtration, washed with water and dried *in vacuo*. This material (1.3 g, 4.5 mmol) was dissolved in ethanol (35 cm<sup>3</sup>) and acetic acid (15 cm<sup>3</sup>). Hydrazine monohydrate (0.68 g, 13.5 mmol) was then added and the mixture stirred at room temperature for 12 hours. The solution was neutralised using aqueous NaOH, and water was added until a precipitate formed which was collected by filtration and washed with water. Yield 0.84 g, 68.0 %. Found C, 66.2; H, 7.00; N, 23.7 %. Calcd. for C<sub>16</sub>H<sub>19</sub>N<sub>5</sub>·0.5H<sub>2</sub>O C; 66.2; H, 6.94; N, 24.1 %. ESMS *m/z* 282.2 ([HL<sup>4</sup>]<sup>+</sup>). <sup>1</sup>H NMR (CDCl<sub>3</sub>) δ 1.39 (s, 9H, C(CH<sub>3</sub>)<sub>3</sub>), 2.37 (s, 3H, CH<sub>3</sub>), 6.55 and 6.63 (both s, 1H, 2x Pz H<sup>4</sup>), 7.53 and 7.60 (both d, 7.5 Hz, 1H, Py H<sup>3</sup> and H<sup>5</sup>), 7.73 (t, 7.5 Hz, 1H, Py H<sup>4</sup>). <sup>13</sup>C NMR (CDCl<sub>3</sub>) δ 12.2 (1C, CH<sub>3</sub>), 30.9 (1C, C(CH<sub>3</sub>)<sub>3</sub>), 32.6 (3C, C(CH<sub>3</sub>)<sub>3</sub>), 101.1 and 104.0 (both 1C, 2x Pz C<sup>4</sup>), 119.8 and 119.9 (both 1C, Py C<sup>3</sup> and C<sup>5</sup>), 138.9 (Py C<sup>4</sup>), 148.1, 151.4 (both br, 1C, 2x Pz C<sup>5</sup>). Other quaternary <sup>13</sup>C resonances not observed, probably because of rapid tautomerism of the pyrazolyl NH groups.<sup>40</sup>

**Synthesis of 2-(5-*tert*-Butyl-1H-pyrazol-3-yl)-6-(5-amino-1H-pyrazol-3-yl)pyridine (L<sup>5</sup>).** Sodium methoxide (1.0 g, 18.3 mmol) and pinacolone (1.8 g, 18.3 mmol) were added to a stirred suspension of dimethyl pyridine-2,6-dicarboxylate (3.0 g, 18.3 mmol) in toluene (150 cm<sup>3</sup>) and the mixture was stirred at 70 °C overnight under dinitrogen. Sodium hydride (60 wt % in mineral oil, 1.1 g, 27.5 mmol) was washed with pentane and transferred to the reaction mixture, followed by acetonitrile (1.1 g, 27.5 mmol). The mixture was then heated to reflux for 4 hrs and then 65 °C for 12 hrs. The solution was cooled and the resultant precipitate was collected by filtration. The solid was redissolved in water and acidified to pH 5 leading to the appearance of a yellow oil which was extracted with chloroform and dried over MgSO<sub>4</sub>. Removal of the solvent afforded 2.5 g of crude 2-(3-hydroxy-4,4-dimethylpent-2-enoyl)-6-(2-cyanoacetyl)pyridine as a yellow oil. This material (2.5 g, 9.3 mmol) was dissolved in 7:3 ethanol:acetic acid (50 cm<sup>3</sup>). Hydrazine hydrate (1.9 g, 37.2 mmol) was then added and the mixture stirred at room temperature for 48 hrs. The solvent was then reduced to half its original volume and neutralised with aqueous NaHCO<sub>3</sub>. The remaining solvent was then removed to leave a sticky orange residue which was sonicated in diethyl ether to afford a white precipitate. Yield 2.3 g, 86.5 %. Found C, 63.3; H, 6.55; N, 29.7 %. Calcd for C<sub>15</sub>H<sub>18</sub>N<sub>6</sub> C, 63.8; H, 6.43; N, 29.8 %. ESMS *m/z* 283.2 ([HL<sup>5</sup>]<sup>+</sup>). <sup>1</sup>H NMR ((CD<sub>3</sub>)<sub>2</sub>SO) δ 1.34 (s, 9H, C(CH<sub>3</sub>)<sub>3</sub>), 6.07 (s, 1H, Pz H<sup>4</sup>) 6.85 (s, 1H, Pz H<sup>4</sup>), 7.61 (d, 7.7 Hz, 1H, Py H<sup>5</sup>), 7.73 (d, 7.6 Hz, 1H, Py H<sup>3</sup>), 7.82 (pseudo-t, 7.6 Hz, 1H, Py H<sup>4</sup>). <sup>13</sup>C NMR ((CD<sub>3</sub>)<sub>2</sub>SO) δ 30.3 (3C, C(CH<sub>3</sub>)<sub>3</sub>), 31.1 (1C, C(CH<sub>3</sub>)<sub>3</sub>), 88.9 (1C, Pz C<sup>4</sup>), 99.8 (1C, Pz C<sup>4</sup>), 117.3 and 117.4 (both 1C, Py C<sup>3</sup> and C<sup>5</sup>), 119.9 and 122.1 (both 1C, 2x Pz C<sup>3</sup>), 137.5 (1C, Py

C<sup>4</sup>), 144.2 and 149.0 (both 1C, 2x Pz C<sup>5</sup>), 154.3 and 156.4 (both 1C, Py C<sup>2</sup> and C<sup>6</sup>).

**Synthesis of [Fe(L<sup>1</sup>)<sub>2</sub>][ClO<sub>4</sub>]<sub>2</sub>·2H<sub>2</sub>O (1[ClO<sub>4</sub>]<sub>2</sub>·2H<sub>2</sub>O).** L<sup>1</sup> (0.20 g, 0.8 mmol) and Fe[ClO<sub>4</sub>]<sub>2</sub>·6H<sub>2</sub>O (0.10 g, 0.4 mmol) were suspended in nitromethane (15 cm<sup>3</sup>). The solution initially adopted a green colouration, which darkened to brown after stirring for 30 mins. The solution was filtered and concentrated to ca. 5 cm<sup>3</sup>. Slow diffusion of diethyl ether vapour into the solution yielded orange crystals that were suitable for X-ray analysis. The crystals were collected and dried *in vacuo*, affording an orange material that analyses as the dihydrate of the desired complex. Yield 0.17 g, 56.6 %. Found C, 34.5; H, 2.80; N, 25.2 %. Calcd. for C<sub>22</sub>H<sub>22</sub>Cl<sub>2</sub>FeN<sub>14</sub>O<sub>8</sub>·2H<sub>2</sub>O C 34.2; H, 3.39; N, 25.4 %. ESMS *m/z* 269.1 ([Fe(L<sup>1</sup>)<sub>2</sub>]<sup>2+</sup>). <sup>1</sup>H NMR (CD<sub>3</sub>NO<sub>2</sub>) δ 9.9 (8H, NH<sub>2</sub>), 27.8 (4 H, Pz NH), 31.2 (2H, Py H<sup>4</sup>), 50.4 and 59.7 (both 4H, Py H<sup>3</sup> and Pz H<sup>4</sup>).

**Synthesis of [Fe(L<sup>2</sup>)<sub>2</sub>][BF<sub>4</sub>]<sub>2</sub>·H<sub>2</sub>O (2[BF<sub>4</sub>]<sub>2</sub>·H<sub>2</sub>O).** A mixture Fe[BF<sub>4</sub>]<sub>2</sub>·6H<sub>2</sub>O (0.06 g, 0.2 mmol) and L<sup>2</sup> (0.13 g, 0.3 mmol) in nitromethane (15 cm<sup>3</sup>) was stirred at room temperature for 30 mins. Diethyl ether was then added until a yellow precipitate formed, which was collected and dried. The product was recrystallized from acetonitrile/diethyl ether. Yield 0.11 g, 66.2 %. Found C, 47.2; H, 5.25; N, 18.1 %. Calcd. for C<sub>42</sub>H<sub>54</sub>B<sub>2</sub>F<sub>8</sub>FeN<sub>14</sub>O<sub>4</sub>·H<sub>2</sub>O C, 47.3; H, 5.29; N, 18.4 %. ESMS *m/z* 410.2 ([HL<sup>2</sup>]<sup>+</sup>). <sup>1</sup>H NMR ({CD<sub>3</sub>}<sub>2</sub>CO) δ 3.0 (36 H, CH<sub>3</sub>), 15.2 (4H, CONH), 24.3 (2H, Py H<sup>4</sup>), 31.4 (4H, Pz NH), 55.0 and 60.3 (both 4H, Py H<sup>3/5</sup> and Pz H<sup>4</sup>).

**Synthesis of [Fe(L<sup>2</sup>)<sub>2</sub>][ClO<sub>4</sub>]<sub>2</sub>·2H<sub>2</sub>O (2[ClO<sub>4</sub>]<sub>2</sub>·2H<sub>2</sub>O).** Method as for [Fe(L<sup>2</sup>)<sub>2</sub>][BF<sub>4</sub>]<sub>2</sub>, using Fe[ClO<sub>4</sub>]<sub>2</sub>·6H<sub>2</sub>O (0.07 g, 0.2 mmol). The product is a yellow solid. Found C, 45.7; H, 5.05; N, 17.8 % Calcd. for C<sub>42</sub>H<sub>54</sub>Cl<sub>2</sub>FeN<sub>14</sub>O<sub>12</sub>·2H<sub>2</sub>O C, 45.5; H, 5.27; N, 17.7 %. ESMS *m/z* 410.2 ([HL<sup>2</sup>]<sup>+</sup>), 432.2 ([NaL<sup>2</sup>]<sup>+</sup>).

**Synthesis of [Fe(L<sup>3</sup>)<sub>2</sub>][BF<sub>4</sub>]<sub>2</sub>·CF<sub>3</sub>CH<sub>2</sub>OH (3[BF<sub>4</sub>]<sub>2</sub>·CF<sub>3</sub>CH<sub>2</sub>OH).** Fe[BF<sub>4</sub>]<sub>2</sub>·6H<sub>2</sub>O (0.10 g, 0.3 mmol) was added to a stirred solution of L<sup>3</sup> (0.20 g, 0.6 mmol) in methanol (15 cm<sup>3</sup>), and the mixture was for 30 mins. The solvent was evaporated to dryness and the brown residue was recrystallised from trifluoroethanol/diethyl ether as the anti-solvent. Yield 0.16 g, 58 %. Found C, 48.8; H, 5.60; N, 14.8 %. Calcd. for C<sub>38</sub>H<sub>50</sub>B<sub>2</sub>F<sub>8</sub>FeN<sub>10</sub>·CF<sub>3</sub>CH<sub>2</sub>OH C 49.2; H, 5.47; N, 14.4 %. The presence of one equivalent of 2,2,2-trifluoroethanol in the dried solid is consistent with the crystal structure of the compound. ESMS *m/z* 701.3 ([Fe(L<sup>3</sup>)<sub>2</sub>]<sup>+</sup>). <sup>1</sup>H NMR ({CD<sub>3</sub>}<sub>2</sub>CO) δ 2.1 (36H, C(CH<sub>3</sub>)<sub>3</sub>), 23.1 (2H, PyH<sup>4</sup>), 35.7 (4H, Pz NH), 53.1 and 59.0 (both 4H, Py H<sup>3/5</sup> and Pz H<sup>4</sup>).

**Synthesis of [Fe(L<sup>4</sup>)<sub>2</sub>][BF<sub>4</sub>]<sub>2</sub>·½CF<sub>3</sub>CH<sub>2</sub>OH (4[BF<sub>4</sub>]<sub>2</sub>·½CF<sub>3</sub>CH<sub>2</sub>OH).** A solution of Fe[BF<sub>4</sub>]<sub>2</sub>·6H<sub>2</sub>O (0.06 g, 0.2 mmol) and L<sup>4</sup> (0.13 g, 0.3 mmol) in methanol (15 cm<sup>3</sup>) was stirred at room temperature for 30 mins. The resultant brown solution was concentrated and water was added until a precipitate formed which was collected by filtration and dried.

Crystals of X-ray quality were obtained by slow of diethyl ether into a solution of the crude material in trifluoroethanol. Yield 0.20 g, 71 %. Found C, 47.3; H, 5.15; N, 16.6 % Calcd. for C<sub>32</sub>H<sub>38</sub>B<sub>2</sub>F<sub>8</sub>FeN<sub>10</sub>·½CF<sub>3</sub>CH<sub>2</sub>OH C, 47.1; H, 4.73; N, 16.6 %. The presence of half an equivalent of 2,2,2-trifluoroethanol in this material is consistent with the crystal structure analysis described below. ESMS *m/z* 282.2 ([HL<sup>4</sup>]<sup>+</sup>). <sup>1</sup>H NMR ({CD<sub>3</sub>}<sub>2</sub>CO) δ 1.9 (18H, C(CH<sub>3</sub>)<sub>3</sub>), 20.6 (6H, CH<sub>3</sub>), 23.0 (s, 2H, Py H<sup>4</sup>), 48.7 and 53.0 (both 2H, Pz H<sup>4</sup>), 56.3 and 60.1 (both 2H, Py H<sup>3</sup> and H<sup>5</sup>).

### Single crystal X-ray structure determinations

The single crystals in this work were grown by vapour diffusion methods, using the following solvent:antisolvent combinations: MeNO<sub>2</sub>:Et<sub>2</sub>O (1[ClO<sub>4</sub>]<sub>2</sub>·2(C<sub>2</sub>H<sub>5</sub>)<sub>2</sub>O·CH<sub>3</sub>NO<sub>2</sub>); MeCN:Et<sub>2</sub>O (2[BF<sub>4</sub>]<sub>2</sub>·3CH<sub>3</sub>CN and 2[ClO<sub>4</sub>]<sub>2</sub>·3CH<sub>3</sub>CN); CF<sub>3</sub>CH<sub>2</sub>OH:*i*Pr<sub>2</sub>O (3[BF<sub>4</sub>]<sub>2</sub>·*x*CF<sub>3</sub>CH<sub>2</sub>OH·*y*({CH<sub>3</sub>}<sub>2</sub>CH)<sub>2</sub>O) and CF<sub>3</sub>CH<sub>2</sub>OH:Et<sub>2</sub>O (4[BF<sub>4</sub>]<sub>2</sub>·*x*CF<sub>3</sub>CH<sub>2</sub>OH·*y*(C<sub>2</sub>H<sub>5</sub>)<sub>2</sub>O). Diffraction data were measured using a Bruker X8 Apex II diffractometer fitted with an Oxford Cryostream low temperature device, using graphite-monochromated Mo-*K*α radiation (λ = 0.71073 Å) generated by a rotating anode. Experimental details of the structure determinations in this study are given in Table 2. All the structures were solved by direct methods (*SHELXS97*<sup>41</sup>), and developed by full least-squares refinement on *F*<sup>2</sup> (*SHELXL97*<sup>41</sup>). Crystallographic figures were prepared using *X-SEED*,<sup>42</sup> which incorporates *POVRAY*.<sup>43</sup>

**X-ray structure refinements.** The asymmetric unit of 1[ClO<sub>4</sub>]<sub>2</sub>·2(C<sub>2</sub>H<sub>5</sub>)<sub>2</sub>O·CH<sub>3</sub>NO<sub>2</sub> contains half a complex dication, with Fe(1) lying on the crystallographic C<sub>2</sub> site ½, *y*, ¼; a perchlorate anion and a diethyl ether molecule, both lying on general crystallographic positions; and, a disordered half-molecule of nitromethane spanning the C<sub>2</sub> axis ½, *y*, ¾. The disordered nitromethane was modelled over two sites of occupancy 0.25, subject to the fixed restraints C–N = 1.48(2), N–O = 1.22(2), O...O = 2.14(2) and C...O = 2.32(2) Å. All non-H atoms except the disordered solvent were refined anisotropically, while C-bound H atoms were placed in calculated positions and refined using a riding model. The N-bound H atoms were all located in the Fourier map and allowed to refine, subject to the refined restraint N–H = 0.84(2) Å.

Isostructural 2[BF<sub>4</sub>]<sub>2</sub>·3CH<sub>3</sub>CN and 2[ClO<sub>4</sub>]<sub>2</sub>·3CH<sub>3</sub>CN contain one formula unit per symmetric unit, and were refined following the same procedure. The same two tertbutyl groups in both structures are disordered. One of these was refined over two half-occupied sites sharing a common wholly occupied bridgehead C atom, while the other was modelled over three orientations with occupancies of 0.50, 0.25 and 0.25. The refined restraints C–C = 1.53(2) and 1,3-C...C = 2.50(2) Å were applied to these groups. All non-H atoms with occupancy ≥0.5 were refined anisotropically, while H atoms were placed in calculated positions and refined using a riding model. The slightly high value of *R*<sub>int</sub> for the perchlorate salt (Table 2) may

reflect a mild twinning of the crystal. This has no apparent effect on the quality of the structure refinement, however.

The asymmetric unit of **3**[BF<sub>4</sub>]<sub>2</sub>·xCF<sub>3</sub>CH<sub>2</sub>OH·y({CH<sub>3</sub>)<sub>2</sub>CH)<sub>2</sub>O (*x* ≈ 0.73, *y* ≈ 0.35) contains two formula units of the compound. That is, two complex dications labelled 'A' and 'B'; four BF<sub>4</sub><sup>-</sup> anions, three partially occupied 2,2,2-trifluoroethanol sites whose occupancies sum to 1.45, and a disordered part-occupied di-*isopropyl* ether molecule with total occupancy 0.7. The solvent occupies channels in the lattice, running parallel to (111). Two *tert*butyl groups in molecule A, and one in molecule B, were modelled as disordered over two equally occupied orientations using the refined restraints C–C = 1.54(2) and 1,3-C...C = 2.51(2) Å. The BF<sub>4</sub><sup>-</sup> anion B(65)-F(69) is also disordered, and was modelled over two orientations sharing a common wholly occupied B atom. The occupancy ratio of the two sites refined to 0.59:0.41, and the refined restraints B–F = 1.39(2) and F...F = 2.27(2) Å were applied to that residue. Slightly high displacement parameters on some other *tert*butyl groups and anions may also indicate a degree of disorder in those residues, but this was not modelled. The three 2,2,2-trifluoroethanol molecules were refined with occupancies of 0.70, 0.50 and 0.25. The latter required the following fixed restraints to refine stably: C–C = 1.52(2), C–O = 1.43(2), C–F = 1.33(2), F...F = 2.17(2), 1,3-C...F = 2.33(2) and 1,3-C...O = 2.40(2) Å. Lastly, the two partial di-*isopropyl* ether sites were refined with occupancies of 0.30 and 0.40, subject to the fixed restraints C–C = 1.52(2), C–O = 1.43(2), 1,3-CH<sub>3</sub>...CH<sub>3</sub> = 2.48(2) and 1,3-

CH...CH = 2.34(2) Å. All non-H atoms with occupancy >0.5 were refined anisotropically, and H atoms were placed in calculated positions and refined using a riding model.

The asymmetric unit of **4**[BF<sub>4</sub>]<sub>2</sub>·xCF<sub>3</sub>CH<sub>2</sub>OH·y(C<sub>2</sub>H<sub>5</sub>)<sub>2</sub>O (*x* ≈ 0.25, *y* ≈ 2.60) contains: one complex dication; two disordered BF<sub>4</sub><sup>-</sup> anions; two fully occupied ordered diethyl ether molecules, one of which is disordered over two half-occupied sites; one complete 0.2-occupied diethyl ether molecule spanning the inversion centre at 0, 0.5, 0.5; and, an additional disordered region that was modelled using partial diethyl ether (occupancy 0.4) and 2,2,2-trifluoroethanol (occupancy 0.25) sites. The disordered anions were each refined over two orientations, whose occupancies each converged to a ratio of 0.66:0.34. These were modelled using the refined restraints B–F = 1.38(2) and F...F = 2.25(2) Å. The following fixed restraints were also applied to the disordered and partly occupied solvent moieties. For diethyl ether: C–C = 1.52(2), C–O = 1.43(2), 1,3-C...C = 2.28(2) and 1,3-C...O = 2.34(2) Å. For 2,2,2-trifluoroethanol: C–C = 1.52(2), C–O = 1.43(2), C–F = 1.38(2), 1,3-C...F = F...F = 2.28(2) and 1,3-C...O = 2.34(2) Å. The displacement ellipsoids on the *tert*butyl C atoms imply that these groups may also be disordered, but attempts to refine this gave unrealistic results. Hence these groups were left as ordered in the final least squares cycles. All non-H atoms with occupancies >0.5 were refined anisotropically, and all H atoms were placed in calculated positions and refined using a riding model.

**Table 2** Experimental details for the single crystal structure determinations in this study.

	<b>1</b> [ClO <sub>4</sub> ] <sub>2</sub> ·- 2(C <sub>2</sub> H <sub>5</sub> ) <sub>2</sub> O·CH <sub>3</sub> NO <sub>2</sub>	<b>2</b> [BF <sub>4</sub> ] <sub>2</sub> ·3CH <sub>3</sub> CN	<b>2</b> [ClO <sub>4</sub> ] <sub>2</sub> ·3CH <sub>3</sub> CN	<b>3</b> [BF <sub>4</sub> ] <sub>2</sub> ·xCF <sub>3</sub> CH <sub>2</sub> OH·- y(C <sub>2</sub> H <sub>5</sub> ) <sub>2</sub> O	<b>4</b> [BF <sub>4</sub> ] <sub>2</sub> ·xCF <sub>3</sub> CH <sub>2</sub> OH·- y(C <sub>2</sub> H <sub>5</sub> ) <sub>2</sub> O
Molecular formula	C <sub>31</sub> H <sub>45</sub> Cl <sub>2</sub> FeN <sub>15</sub> O <sub>12</sub>	C <sub>48</sub> H <sub>63</sub> B <sub>2</sub> F <sub>8</sub> FeN <sub>17</sub> O <sub>4</sub>	C <sub>48</sub> H <sub>63</sub> Cl <sub>2</sub> FeN <sub>17</sub> O <sub>12</sub>	C <sub>41.55</sub> H <sub>57.08</sub> B <sub>2</sub> F <sub>10.18</sub> FeN <sub>10</sub> O <sub>1.08</sub>	C <sub>42.90</sub> H <sub>64.75</sub> B <sub>2</sub> F <sub>8.75</sub> FeN <sub>10</sub> O <sub>2.85</sub>
<i>M<sub>r</sub></i>	946.57	1171.62	1196.90	984.64	1009.92
Crystal class	orthorhombic	triclinic	triclinic	orthorhombic	monoclinic
Space group	<i>Pbcn</i>	<i>P</i> $\bar{1}$	<i>P</i> $\bar{1}$	<i>P2<sub>1</sub>2<sub>1</sub>2<sub>1</sub></i>	<i>P2<sub>1</sub>/c</i>
<i>a</i> (Å)	14.5138(7)	12.8890(4)	12.995(2)	17.588(2)	15.1739(5)
<i>b</i> (Å)	23.2609(11)	13.3521(4)	13.3971(19)	19.509(2)	17.9832(6)
<i>c</i> (Å)	12.8419(6)	19.1548(6)	19.304(3)	32.399(5)	19.9978(7)
$\alpha$ (°)	–	104.759(2)	104.696(7)	–	–
$\beta$ (°)	–	100.581(2)	100.401(9)	–	95.1170(10)
$\gamma$ (°)	–	108.536(2)	108.320(8)	–	–
<i>V</i> (Å <sup>3</sup> )	4335.5(4)	2893.71(15)	2959.6(8)	11117(3)	5435.2(3)
<i>Z</i>	4	2	2	8	4
$\mu$ (Mo–K $\alpha$ ) (mm <sup>-1</sup> )	0.546	0.343	0.416	0.343	0.352
<i>T</i> (K)	150(2)	150(2)	150(2)	150(2)	110(2)
Measured reflections	58012	61654	67966	124468	58452
Independent reflections	5826	20577	17432	20237	13077
<i>R</i> <sub>int</sub>	0.040	0.052	0.110	0.057	0.037
<i>R</i> <sub>1</sub> , <i>I</i> > 2 $\sigma$ ( <i>I</i> ) <sup>a</sup>	0.034	0.048	0.064	0.065	0.078
<i>wR</i> <sub>2</sub> , all data <sup>b</sup>	0.092	0.129	0.177	0.193	0.263
Goodness of fit	1.056	1.021	1.027	1.045	1.055
Flack parameter	–	–	–	–0.002(15)	–

$$^a R = \sum [|F_o| - |F_c|] / \sum |F_o| \quad ^b wR = [\sum w(F_o^2 - F_c^2) / \sum wF_o^4]^{1/2}$$

## Other measurements

Elemental microanalyses were performed by the University of Leeds School of Chemistry microanalytical service. Electrospray mass spectra (ESMS) were obtained on a Bruker MicroTOF spectrometer, from MeCN feed solutions. All mass peaks have the correct isotopic distributions for the proposed assignments.

Magnetic susceptibility measurements were performed on a Quantum Design VSM SQUID magnetometer, in an applied field of 5000 G. A diamagnetic correction for the sample was estimated from Pascal's constants,<sup>44</sup> a diamagnetic correction for the sample holder was also measured, and applied to the data.

## Acknowledgements

This work was funded by the University of Leeds (Brotherton Scholarship to TDR) and the EPSRC. The authors thank Colin Kilner (School of Chemistry, University of Leeds) for help with some of the crystal structure determinations, and Drs Oscar Cespedes (School of Physics and Astronomy, University of Leeds) and Floriana Tuna (Photon Science Institute, University of Manchester) for assistance with the magnetic susceptibility measurements.

## Notes and references

<sup>a</sup>School of Chemistry, University of Leeds, Woodhouse Lane, Leeds, UK LS2 9JT. E-mail: m.a.halcrow@leeds.ac.uk; Fax: +44 113 343 6565; Tel: +44 113 343 6506.

<sup>b</sup>Current address: Department of Chemistry, University of Liverpool, Crown Street, Liverpool, UK L69 7ZD

† Electronic Supplementary Information (ESI) available: additional crystallographic Figures and Tables, and magnetic susceptibility data. CCDC 982126–982130. For ESI and crystallographic data in CIF or other electronic format see DOI: 10.1039/#####.

- 1 P. Gülich and H. A. Goodwin (eds.), *Spin Crossover in Transition Metal Compounds I-III*, *Top. Curr. Chem.*, 2004, **233-235**.
- 2 M. A. Halcrow (ed), *Spin-crossover materials - properties and applications*, John Wiley & Sons, Chichester, 2013, p. 568.
- 3 A. Bousseksou, G. Molnár, L. Salmon and W. Nicolazzi, *Chem. Soc. Rev.*, 2011, **40**, 3313.
- 4 M. A. Halcrow, *Chem. Soc. Rev.*, 2011, **40**, 4119.
- 5 P. Guionneau, *Dalton Trans.*, 2014, **43**, 382.
- 6 J.-F. Létard, *J. Mater. Chem.*, 2006, **16**, 2550; J. A. Wolny, R. Diller and V. Schünemann, *Eur. J. Inorg. Chem.*, 2012, 2635; M. Sorai, Y. Nakazawa, M. Nakano and Y. Miyazaki, *Chem. Rev.*, 2013, **113**, PR41.
- 7 For other recent reviews see: P. Gamez, J. S. Costa, M. Quesada and G. Aromí, *Dalton Trans.*, 2009, 7845; M. C. Muñoz and J. A. Real, *Coord. Chem. Rev.*, 2011, **255**, 2068; J. Tao, R.-J. Wei, R.-B. Huang and L.-S. Zheng, *Chem. Soc. Rev.*, 2012, **41**, 703; P. Gülich, *Eur. J. Inorg. Chem.*, 2013, 581.
- 8 M. A. Halcrow, *Coord. Chem. Rev.*, 2005, **249**, 2880; J. Olguín and S. Brooker, *Coord. Chem. Rev.*, 2011, **255**, 203.
- 9 M. A. Halcrow, *New J. Chem.*, in the press (doi: 10.1039/c3nj00835e).
- 10 See e.g. K. H. Sugiyarto, D. C. Craig, A. D. Rae and H. A. Goodwin, *Aust. J. Chem.*, 1994, **47**, 869. M. Clemente-León, E. Coronado, M. C. Giménez-López, F. M. Romero, S. Asthana, C. Desplanches and J.-F. Létard, *Dalton Trans.*, 2009, 8087.
- 11 T. D. Roberts, F. Tuna, T. L. Malkin, C. A. Kilner and M. A. Halcrow, *Chem. Sci.*, 2012, **3**, 349; T. D. Roberts, M. A. Little, F. Tuna, C. A. Kilner and M. A. Halcrow, *Chem. Commun.*, 2013, **49**, 6280.
- 12 S. A. Barrett, C. A. Kilner and M. A. Halcrow, *Dalton Trans.*, 2011, **40**, 12021.
- 13 S. A. Barrett and M. A. Halcrow, *RSC Adv.*, 2014, **4**, 11240.
- 14 See e.g. T. Jozak, D. Zabel, A. Schubert, Y. Sun and W. R. Thiel, *Eur. J. Inorg. Chem.*, 2010, 5135; S. Günnaz, N. Özdemir, S. Dayan, O. Dayan and B. Çetinkaya, *Organometallics*, 2011, **30**, 4165; Q. Yang, L. Wang, L. Lei, X.-L. Zheng, H. Fu, M. Yuan, H. Chen and R.-X. Li, *Catal. Commun.*, 2012, **29**, 194; K. Umehara, S. Kuwata and T. Ikariya, *J. Am. Chem. Soc.*, 2013, **135**, 6754.
- 15 C.-C. Chou, K.-L. Wu, Y. Chi, W.-P. Hu, S. J. Yu, G.-H. Lee, C.-L. Lin, and P.-T. Chou, *Angew. Chem. Int. Ed.*, 2011, **50**, 2054; K.-L. Wu, C.-H. Li, Y. Chi, J. N. Clifford, L. Cabau, E. Palomares, Y.-M. Chengm H.-A. Pan and P.-T. Chou, *J. Am. Chem. Soc.*, 2012, **134**, 7488.
- 16 See e.g. T. R. Scicluna, B. H. Fraser, N. T. Gorham, J. G. MacLellan, M. Massi, B. W. Skelton, T. G. St Pierre and R. C. Woodward, *CrystEngComm*, 2010, **12**, 3422; J. S. Costa, G. A. Craig, L. A. Barrios, O. Roubeau, E. Ruiz, S. Gómez-Coca, S. J. Teat and G. Aromí, *Chem. Eur. J.*, 2011, **17**, 4960; G. N. Newton, T. Onuki, T. Shiga, M. Noguchi, T. Matsumoto, J. S. Mathieson, M. Nihei, M. Nakano, L. Cronin and H. Oshio, *Angew. Chem. Int. Ed.*, 2011, **50**, 4844; Shiga, M. Noguchi, H. Sato, T. Matsumoto, G. N. Newton and H. Oshio, *Dalton Trans.*, 2013, **42**, 16185; H. Sato, L. Miya, K. Mitsumoto, T. Matsumoto, T. Shiga, G. N. Newton and H. Oshio, *Inorg. Chem.*, 2013, **52**, 9714.
- 17 G. A. Craig, J. S. Costa, O. Roubeau, S. J. Teat and G. Aromí, *Chem. Eur. J.*, 2011, **17**, 3120; G. A. Craig, J. S. Costa, S. J. Teat, O. Roubeau, D. S. Yufit, J. A. K. Howard and G. Aromí, *Inorg. Chem.*, 2013, **52**, 7203; J. S. Costa, S. Rodríguez-Jiménez, G. A. Craig, B. Barth, C. M. Beavers, S. J. Teat and G. Aromí, *J. Am. Chem. Soc.* 2014, **136**, 3869.
- 18 M. C. Etter, *Acc. Chem. Res.*, 1990, **23**, 120.
- 19 C. M. Pask, K. D. Camm, N. J. Bullen, M. J. Carr, W. Clegg, C. A. Kilner and M. A. Halcrow, *Dalton Trans.*, 2006, 662; C. M. Pask, K. D. Camm, C. A. Kilner and M. A. Halcrow, *Tetrahedron Lett.*, 2006, **47**, 2531; L. F. Jones, K. D. Camm, C. A. Kilner and M. A. Halcrow, *CrystEngComm*, 2006, **8**, 719.
- 20 S. Sengupta and R. Mondal, *Chem. Eur. J.*, 2013, **19**, 5537; L.-A. Chen, W. Xu, B. Huang, J. Ma, L. Wang, J. Xi, K. Harms, L. Gong and E. Meggers, *J. Am. Chem. Soc.*, 2013, **135**, 10598; N. Zarrabi, J. J. Hayward, W. Clegg and M. Pilkington, *Dalton Trans.* 2014, **43**, 2352.
- 21 X. Liu, J. A. McAllister, M. P. de Miranda, B. J. Whitaker, C. A. Kilner, M. Thornton-Pett and M. A. Halcrow, *Angew. Chem., Int. Ed.*, 2002, **41**, 756; X. Liu, A. C. McLaughlin, M. P. de Miranda, E. J. L. McInnes, C. A. Kilner and M. A. Halcrow, *Chem. Commun.*,

- 2002, 2978; X. Liu, J. A. McAllister, M. P. de Miranda, E. J. L. McInnes, C. A. Kilner and M. A. Halcrow, *Chem. Eur. J.*, 2004, **10**, 1827.
- 22 X. Liu, C. A. Kilner and M. A. Halcrow, *Chem. Commun.*, 2002, 704; S. L. Renard, C. A. Kilner, J. Fisher and M. A. Halcrow, *J. Chem. Soc., Dalton Trans.*, 2002, 4206; S. L. Renard, A. Franken, C. A. Kilner, J. D. Kennedy and M. A. Halcrow, *New J. Chem.*, 2002, **26**, 1634; S. L. Renard, I. Sylvestre, S. A. Barrett, C. A. Kilner and M. A. Halcrow, *Inorg. Chem.*, 2006, **45**, 8711.
- 23 L. F. Jones, C. A. Kilner, M. P. de Miranda, J. Wolowska and M. A. Halcrow, *Angew. Chem., Int. Ed.*, 2007, **46**, 407; L. F. Jones, S. A. Barrett, C. A. Kilner and M. A. Halcrow, *Chem. Eur. J.*, 2008, **14**, 223; L. F. Jones, C. A. Kilner and M. A. Halcrow, *Chem. Eur. J.*, 2009, **15**, 4667; J. J. Henkelis, L. F. Jones, C. A. Kilner and M. A. Halcrow, *Inorg. Chem.*, 2010, **49**, 11127; J. J. Henkelis, C. A. Kilner and M. A. Halcrow, *Chem. Commun.*, 2011, **47**, 5187.
- 24 K. A. Ali, *ARKIVOC*, 2010, (xi), 55.
- 25 A. Yoshinari, A. Tazawa, S. Kuwata and T. Ikariya, *Chem. Asian J.*, 2012, **7**, 1417.
- 26 C. T. Brewer, G. Brewer, R. J. Butcher, E. E. Carpenter, A. M. Schmierekamp and C. Viragh, *Dalton Trans.*, 2007, 295.
- 27 H. Z. Lazar, T. Forestier, S. A. Barrett, C. A. Kilner, J.-F. Létard and M. A. Halcrow, *Dalton Trans.*, 2007, 4276.
- 28 J.-L. M. Abboud, J. P. Cabildo, T. Cañada, J. Catalán, R. M. Claramunt, J. L. G. de Paz, J. Elguero, J. H. Homan, R. Notario, C. Toiron and G. I. Yranzo, *J. Org. Chem.*, 1992, **57**, 3938.
- 29 L. Öhrström and K. Larsson, *Molecule-Based Materials – the Structural Network Approach*, Elsevier, Amsterdam, 2005, p. 314.
- 30 H. Chun, D. Kim, D. N. Dybtsev and K. Kim, *Angew. Chem., Int. Ed.*, 2004, **43**, 971; S.-L. Li, Y.-Q. Lan, J.-S. Qin, J.-F. Ma and Z.-M. Su, *Cryst. Growth Des.*, 2008, **8**, 2055; Z. Zheng, R. Wu, J. Li and Y. Sun, *J. Coord. Chem.*, 2009, **62**, 2324; C.-H. Zhan, M.-X. Jiang, Y.-L. Feng and J.-W. Cheng, *CrystEngComm*, 2010, **12**, 420; J. M. Gotthardt, K. F. White, B. F. Abrahams, C. Ritchie and C. Boskovic, *Cryst. Growth Des.*, 2012, **12**, 4425; D.-J. Zhang, R.-C. Zhang, J.-J. Wang, W.-Z. Qiao and X.-M. Jing, *Inorg. Chem. Commun.*, 2013, **32**, 47.
- 31 Y. Kawakami, Y. Sakuma, T. Wakuda, T. Nakai, M. Shirasaka and Y. Kabe, *Organometallics*, 2010, **29**, 3281.
- 32 J. Elhaïk, C. A. Kilner and M. A. Halcrow, *Dalton Trans.*, 2006, 823; L. J. Kershaw Cook, F. Tuna and M. A. Halcrow, *Dalton Trans.*, 2013, **42**, 2254.
- 33 See e.g. B. F. Abrahams, S. R. Batten, H. Hamit, B. F. Hoskins and R. Robson, *J. Chem. Soc., Chem. Commun.*, 1996, 1313; L. Carlucci, G. Ciani, D. M. Proserpio and A. Sironi, *J. Chem. Soc., Chem. Commun.*, 1996, 1393; T. J. Prior and M. J. Rosseinsky, *Inorg. Chem.*, 2003, **42**, 1564; A. Johansson, M. Håkansson and S. Jagner, *Chem. Eur. J.*, 2005, **11**, 5311; A. B. Lysenko, E. V. Govor, H. Krautscheid and K. V. Domasevitch, *Dalton Trans.*, 2006, 3772; H. Wu, J. Yang, Z.-M. Su, S. R. Batten and J.-F. Ma, *J. Am. Chem. Soc.*, 2011, **133**, 11406; J.-H. Wang, M. Li and D. Li, *Chem. Sci.*, 2013, **4**, 1793; D. Sun, Z.-H. Yan, V. A. Blatov, L. Wang and D.-F. Sun, *Cryst. Growth Des.*, 2013, **13**, 1277.
- 34 J. M. Holland, J. A. McAllister, C. A. Kilner, M. Thornton-Pett, A. J. Bridgeman and M. A. Halcrow, *J. Chem. Soc., Dalton Trans.*, 2002, 548.
- 35 M. Clemente-León, E. Coronado, M. C. Giménez-López, F. M. Romero, *Inorg. Chem.*, 2007, **46**, 11266; G. A. Craig, J. S. Costa, O. Roubeau, S. J. Teat and G. Aromí, *Chem. Eur. J.*, 2012, **18**, 11703; T. D. Roberts, M. A. Little, L. J. Kershaw Cook, S. A. Barrett, F. Tuna and M. A. Halcrow, *Polyhedron*, 2013, **64**, 4.
- 36 M. A. Halcrow, *Coord. Chem. Rev.*, 2009, **253**, 2493.
- 37 E. C. Constable, G. Baum, E. Bill, R. Dyson, R. van Eldik, D. Fenske, S. Kaderli, D. Morris, A. Neubrand, M. Neuburger, D. R. Smith, K. Wiegardt, M. Zehnder and A. D. Zuberbühler, *Chem. Eur. J.*, 1999, **5**, 498; F. Pelascini, M. Wesolek, F. Peruch, A. De Cian, N. Kyritsakas, P. J. Lutz and J. Kress, *Polyhedron*, 2004, **23**, 3193; S. Y. Brauchli, E. C. Constable, K. Harris, D. Häüssinger, C. E. Housecroft, P. J. Rösel and J. A. Zampese, *Dalton Trans.*, 2010, **39**, 10739.
- 38 J. K. McCusker, A. L. Rheingold and D. N. Hendrickson, *Inorg. Chem.*, 1996, **35**, 2100; P. Guionneau, M. Marchivie, G. Bravic, J.-F. Létard and D. Chasseau, *Top. Curr. Chem.*, 2004, **234**, 97.
- 39 Iron(III) complexes of azolate chelates, derived by air-induced oxidation of iron(II) precursors, can be spin-crossover active. See ref. 26, and: Y. Sunatsuki, Y. Ikuta, N. Matsumoto, H. Ohta, M. Kojima, S. Iijima, S. Hayami, Y. Maeda, S. Kaizaki, F. Dahan and J.-P. Tuchagues, *Angew. Chem. Int. Ed.*, 2003, **42**, 1614; Y. Sunatsuki, H. Ohta, M. Kojima, Y. Ikuta, Y. Goto, N. Matsumoto, S. Iijima, H. Akashi, S. Kaizaki, F. Dahan and J.-P. Tuchagues, *Inorg. Chem.*, 2004, **43**, 4154; C. Cook, F. Habib, T. Aharen, R. Clérac, A. Hu and M. Murugesu, *Inorg. Chem.*, 2013, **52**, 1825.
- 40 R. M. Claramunt, C. López, M. D. Santa María, D. Sanz and J. Elguero, *Prog. Nucl. Magn. Reson. Spectr.*, 2006, **49**, 169.
- 41 G. M. Sheldrick, *Acta Crystallogr., Sect. A*, 2008, **64**, 112
- 42 L. J. Barbour, *J. Supramol. Chem.*, 2001, **1**, 189.
- 43 *POVRAY*, v. 3.5, Persistence of Vision Raytracer Pty. Ltd., Williamstown, Victoria, Australia, 2002. <http://www.povray.org>.
- 44 C. J. O'Connor, *Prog. Inorg. Chem.*, 1982, **29**, 203.